

Published in final edited form as:

Biomacromolecules. 2011 May 9; 12(5): 1428–1437. doi:10.1021/bm101192b.

***In situ* Gelable Interpenetrating Double Network Hydrogel Formulated from Binary Components: Thiolated Chitosan and Oxidized Dextran**

Hanwei Zhang, Aisha Qadeer, and Weiliam Chen*

Abstract

In situ gelable interpenetrating double network hydrogels composed of thiolated chitosan (Chitosan-NAC) and oxidized dextran (Odex), completely devoid of potentially cytotoxic small molecule crosslinkers and do not require complex maneuvers or catalysis, have been formulated. The interpenetrating network structure is created by Schiff base formations and disulfide bond inter-crosslinkings through exploiting the disparity of their reaction times. Compare to the auto-gelable thiolated chitosan hydrogels that typically require a relatively long time span for gelation to occur, the Odex/Chitosan-NAC composition solidifies rapidly and forms a well-developed three-dimensional network in a short time span. Compare to typical hydrogels derived from natural materials, the Odex/Chitosan-NAC hydrogels are mechanically strong and resist degradation. The cytotoxicity potential of the hydrogels was determined by an *in vitro* viability assay using fibroblast as a model cell and the results reveal that the hydrogels are non-cytotoxic. In parallel, *in vivo* results from subdermal implantation in mice models demonstrate that this hydrogel is not only highly resistant to degradation but also induces very mild tissue response.

Keywords

In situ gelable; Double interpenetrating network hydrogels; Thiolated chitosan (Chitosan-NAC); Oxidized dextran (Odex)

Introduction

Hydrogels are crosslinked hydrophilic polymer networks capable of absorbing water multiple times of their dry weights, thus, emulating some of the physical characteristics of soft tissues [1–6]. Hydrogels have been utilized in a wide range of biomedical applications including drug/protein delivery [7, 8], contact lenses [9], corneal implants [10], and as scaffolds for tissue engineering [11–15].

In situ gelable hydrogels are advantageous and preferable for medical applications as they can be deployed by injection instead of surgical implantation [16, 17]. The typical obstacles for formulating *in situ* gelable hydrogels for *in vivo* use include gelation occurring at a physiologically acceptable temperature range within a reasonable time span; all components must be non-cytotoxic and perform in a moist and oxygen-rich environment. Much effort has been focused on adapting both natural and synthetic polymers to produce *in situ* gelable hydrogel systems [15–20]. As the regulatory hurdle for natural polymers, especially those with GRAS (Generally Recognized As Safe) designation, is lower than that of their synthetic counterparts, hydrogels formulated entirely from natural polymers are advantageous [15–17,

*Corresponding Author: Weiliam Chen, Division of Wound Healing and Regenerative Medicine, NBV-15N1, Department of Surgery, New York University School of Medicine, New York, NY10016, Tel: 212-263-3002, Fax: 212-263-8216, weiliam.chen@nyumc.org.

20]. We have previously reported *in situ* gelable hydrogels composed of minimally modified natural GRAS materials [6, 16]. However, the mechanical strengths of these hydrogels are relatively low, they also degrade relatively rapidly.

Interpenetrating double networks (DN) is an effective strategy to enhance the mechanical strength of hydrogels [11, 21–25], and their resistance to degradation. Current double networks hydrogels aiming for biomedical uses are consisted largely of synthetic polymers [21–24], using potentially cytotoxic small molecule crosslinkers [24, 25], and also involve complex formulation maneuvers or catalysis [11, 21]. Moreover, significant inflammatory response was observed in *in vivo* implants rendering these hydrogels less suitable for biomedical applications [23]. We have recently reported a hybrid DN two-step photocrosslinked hydrogels composed of *N,N*-dimethylacrylamide and modified hyaluronan, which possesses great mechanical properties [11]. It has not hitherto been reports describing double networks hydrogels derived wholly from natural materials, completely devoid of using small molecule crosslinkers and performing complex formulation maneuvers or catalysis, and prepared in a one-step process.

In this investigation, we demonstrated the feasibility of formulating a class of *in situ* gelable binary interpenetrating double network hydrogels from minimally modified natural GRAS materials, namely, thiolated chitosan and partially oxidized dextran (Odex), in a one-step process without using small molecule crosslinkers. Thiolated chitosan, a water-soluble and minimally modified chitosan derivative, has been shown to form an auto-gelable hydrogel via forming disulfide bonds, and their potential as drug/protein carriers have been studied [26–28]. Importantly, disulfide bonds are very stable under physiological environment (pH=7.4) and effectively resist hydrolysis [29, 30]. Nonetheless, the relatively long gelation time in conjunction with the weak mechanical strength of the hydrogel formed render it less appealing for biomedical applications. We have previously shown the feasibility of forming a rapidly gelable hydrogel by reacting carboxyethylchitosan with Odex via Schiff base formation [6]; the amino residues on the thiolated chitosan enables it to react with Odex in a comparable manner to form a rapidly *in situ* gelable hydrogel. Subsequent reaction between the sulfhydryl residues to form disulfide crosslinks, as a slower process, establishes an interpenetrating double network hydrogel. The structure, gelation mechanism, non-cytotoxicity and degradability of the hydrogel systems were presented and discussed. This interpenetrating double network structure greatly improved the mechanical properties and gelation performance of the hydrogel formulated from thiolated chitosan. The results of *in vivo* subdermal implantation in mice model showed that this hydrogel was not only highly resistant to biodegradation but also only induced very mild tissue response.

2. Experiments

2.1. Materials

Dextran (from *Leuconostoc mesenteroides*, $M_w=76,000$), chitosan (deacetylation degree 85%, M_w 750,000), sodium periodate, N-acetyl-L-cysteine (NAC), 1-ethyl-3-(3-dimethylaminopropyl-carbodiimide) hydrochloride (EDAC), were purchased from Sigma-Aldrich (St. Louis, MO). Dialysis tubings (MWCO 3,500 and 6,000) were from Thermo-Fisher (Hampton, NH). Cell culture inserts (polycarbonate, 6.5 mm diameter, 0.2 μ m pore size) were purchased from NUNC (Rochester, NY). M. DUNNI (clone III8C) murine dermal fibroblast CRL-2017 and McCoy's 5A medium were from ATCC (Manassas, VA). Fetal Bovine Serum (FBS) was acquired from Hyclone (Logan, UT) and Penicillin-Streptomycin (Pen-Strep) solution was from Gibco (Grand Island, NY). MTS assay kit (CellTiter™ 96s) was from Promega (Madison, WI). "Live/Dead™" staining kit was purchased from Molecular Probes (Eugene, OR). All other chemicals were of reagent grade and deionized and distilled water was used.

2.2 Methods

2.2.1 Synthesis of thiolated chitosan (Chitosan-NAC) and oxidized dextran (Odex)

—Chitosan-NAC conjugates were prepared according to the methodologies described by Krauland et al [31]. In brief, 1 g of chitosan was dispersed in water (100 ml), and sufficient HCl was instilled into the chitosan suspension under stirring until a clear solution was obtained. NAC (10, 20, 30, 40 or 60 mmole) was added to the chitosan solution, after adding an EDAC solution (20 mmole), the pH of the reaction mixture was adjusted to 5 with 1M NaOH and diluted to 200 ml; it was then incubated for 3 h at room temperature under agitation. The reaction product was dialyzed (MWCO 6,000) against 5 mM HCl for 1 day, shielded from light, and then 5 mM HCl/1% NaCl for 1 days and finally 1 mM HCl for 1 day. The dialyzed products were then lyophilized and stored at 4 °C before use. The thiol group content of the thiolated chitosan synthesized was determined by elemental analysis and the total amounts of thiol groups were calculated as the weight percentage of sulfur in the polymers. The structures of the thiolated chitosan were determined by ¹H NMR and compared with native chitosan. The data for thiolated chitosan: ¹H NMR (400 MHz, D₂O, TMS, ppm): 4.93(H-1), 3.98(H-3, H-4), 3.81(H-5, H-6), 3.24(H-2), 2.97(-S-CH₂-), 2.07(-COCH₃).

Odex was prepared according to the following process: 3.28 g of NaIO₄ (dissolved in 100 ml of water) was added to 400 ml of dextran solution (1.25% w/v), shielded from light, with constant stirring at ambient temperature for 24 h, an equimolar amount of diethylene glycol was added to quench the unreacted NaIO₄. The Odex solution was dialyzed exhaustively (MWCO 3,500) for 3 days against water, and pure Odex was obtained by lyophilization [32]. The oxidation degree of Odex was determined by quantifying the aldehyde groups formed with tert-butyl carbazate via carbazone formation [6]. The actual oxidation degree of dextran was determined as 20%.

2.2.2 Preparation of solutions and hydrogels—Desired amounts of Odex (5% w/v) and Chitosan-NAC (2.5% w/v) were dissolved in water to form solutions, respectively; and stored at 5 °C before testing. Typical Odex/Chitosan-NAC hydrogels were prepared by thoroughly mixing Odex solutions with Chitosan-NAC solutions (the volume ratio of Odex/Chitosan-NAC was 1:1) by gentle stirring for 10s, the mixture was maintained at 37 °C for gelation.

2.2.3 Physicochemical characterizations of Odex/Chitosan-NAC hydrogels

—All rheological measurements were performed with a rheometer (HAAKE RS600, Thermo-Fisher, Hampton, NH). Liquid samples were transferred into a Couette cell immediately after mixing (time $t=0$). For time sweeping tests, storage moduli G' , loss moduli G'' and viscosity were monitored as a function of time at a 1 Hz frequency and a 2% stress strain under 37 °C. In this investigation, the influence of thiol group contents on chitosan-NAC and its effect on the hydrogels' rheological properties was studied in details.

The burst strengths of hydrogel samples were tested by a custom-built mechanical burst tester following the standard protocol F2392-4 described by ASTM International [33]. Briefly, a sheet of tissue-mimicking collagenous substrate (sausage casing, Nippi Casing Co., Tokyo, Japan) with a 3 mm diameter hole bored in the middle was mounted inside a polytetrafluoroethylene (PTFE) mold (3.0 cm in diameter); 0.6 ml of the hydrogel precursor mix was deposited on the collagenous substrate confined by the PTFE mold to congeal. After incubation for 0.25, 0.5, 1, 3 and 6 hours, respectively, at 37 °C, the hydrogel-substrate was mounted onto the pressurization unit of the tester. This was followed by activating the syringe pump linked to the pressurization unit and a transducer, pressurization was initiated (at 2 ml/min) and the maximum pressure reached immediately prior to material failure was

digitally recorded and registered on a computer. The burst pressure recorded as psi was converted to mmHg using the following formula: Pressure in mmHg/mm thickness = (Pressure in psi×51)/Thickness (mm) of Hydrogel Swelling studies of different Odex/Chitosan-NAC hydrogels were performed in pH 7.4 buffer solutions at 37°C. The weights of the lyophilized hydrogels were recorded (W_d) prior to immersion in PBS. After a stipulated duration of incubation, the hydrogels were blotted with tissue paper to remove excess water, then, they were weighed (W_s). The swelling ratio (q) was calculated by $q = W_s/W_d$.

Both the lyophilized and fractured pieces of hydrogels were secured on an aluminum stub with copper tapes and sputtered with gold, and their cross-sectional morphologies were examined by a scanning electron microscope (SFEGLeo 1550, AMO GmbH, Aachen; Germany) at 10 kV.

2.2.4. Interaction of fibroblast and Odex/Chitosan-NAC hydrogel—Dermal fibroblasts were used as model cells to evaluate the *in vitro* cytotoxicity potential of the Odex/Chitosan-NAC hydrogel formulated, with a secondary objective of verifying the cell-hydrogel interactions. Since the *in situ* gelable Odex/Chitosan-NAC system has potential *in vivo* applications, direct contact cell-hydrogel interaction via encapsulation would be a proper *in vitro* model to evaluate the material. Briefly, Odex (5%) and Chitosan-NAC solutions (2.5%) were pre-sterilized by autoclaving for 10 minutes. 0.2 ml of Odex and Chitosan-NAC solutions and fibroblasts were introduced into each well (cell density: 1×10^5 cells/ml) and the admixture was incubated at 37 °C under a humidified atmosphere of 5% CO₂ for 20 min. Fresh culture medium was then added to the culture well for equilibration and it was repeated thrice in 15 min. Finally, 0.5 ml of cell culture medium was added to each well and the medium was changed every other day.

The cytotoxicity potential of the Odex/Chitosan-NAC hydrogels and their degradation byproducts were determined by MTS assay using the cell-encapsulated hydrogel models; monolayer cells were used as controls. Cell viability was determined on day 0, 3, 7, 14 and 28, respectively. The culture media were removed from individual wells after incubation, 20 µl of MTS solution was added to them, the absorbance of the media were determined at 490 nm following the manufacturer supplied protocol.

To observe cell morphology and proliferation inside the hydrogels, images of cells were acquired *in situ* with a Zeiss laser scanning confocal microscope (LSM510, Carl Zeiss Inc., Germany). The viability of cells in direct contact with the hydrogels was verified by Live/Dead™ staining. Briefly, a fresh cross-section (200 µm) of the cell-laden hydrogel was incubated in 200 µL of a “Live/Dead™” dye solution (2 µM calcein AM and 4µM EthD-1) for 10 min, and it was observed under the scanning confocal microscope. Evaluations of the *in vitro* degradation of hydrogels were also performed with the cell encapsulation model. After incubating for the time-spans ranging from 0 to 28 days, the cell-laden hydrogels were retrieved; the rate of hydrogel degradation was determined by monitoring their weight losses.

2.2.5. Subdermal implantation of Odex/Chitosan-NAC hydrogel—The biocompatibility of the hydrogel and its capacity to resist degradation was evaluated *in vivo* using a mouse subcutaneous implant model. The study was performed according to the approved protocol (#1286) by the IACUC of SUNY-Stony Brook in compliance with the NIH guidelines for the care and use of laboratory animals (NIH Publication no. 85-23 Rev. 1985). Anesthesia was induced by inhalation of isoflurane (5% induction/2.5% maintenance), the injection sites were prepped with both betadine and isopropanol. The precursors (Gel 4) were loaded separately into two syringes and rapidly mixed thoroughly via a two-way connector, a needle was immediately coupled to the syringe containing the

mixed precursor, and the whole process was completed within 15 seconds. The needle was then inserted subdermally into an animal, and 0.5 ml of the hydrogel precursor was introduced into the subdermal pouches formed by gradual dissection under pressurization during injection; injection of each animal took no more than 10 seconds. The animals were euthanized after 7 and 28 days, respectively, and the injection sites in conjunction with the adjoining tissues were retrieved, fixed in 10% neutral buffered formalin, processed for paraffin sectioning, and stained with H&E.

2.3 Statistical analysis

Data were analyzed by ANOVA to evaluate difference between groups. Post hoc comparison of means was accomplished with Student-Newman-Keuls test to determine significance between groups ($\alpha=0.05$).

3. Results and discussion

Reacting chitosan with N-acetyl-L-cysteine forms chitosan-NAC and it has both $-NH_2$ and $-SH$ groups; partial oxidation of dextran with periodate converts some of its vicinal $-OH$ groups into $-CHO$ functionalities. Theoretically, Odex serves as a highly effective macromolecular crosslinker capable of reacting with the free $-NH_2$ groups on the chitosan-NAC; the relatively fast formation of Schiff base results in creating the first crosslinked network. This is followed by the slower interaction of the $-SH$ groups to form disulfide bonds leading to the establishment of a second network. The concept of formation of the hydrogel is depicted in scheme 1. By taking advantage of the disparity in their reaction times, the double interpenetrating network hydrogel is formed by simply blending the two components, as a one step process, without the need to perform any complicated maneuvering.

3.1. Synthesis and characterization of Chitosan-NAC conjugate

Conjugation of NAC to chitosan was achieved by covalent attachment of NAC to the amine groups of the chitosan. The structure of chitosan-NAC was confirmed by the 1H NMR spectrum in D_2O depicted in Figure 1. Compared with the spectrum of chitosan [8], a new resonance peak at 2.97 ppm appeared indicating the presence of a methylene ($-CH_2-SH$) side group.

The actual thiol content (mole %) of Chitosan-NAC could be calculated according to the weight percentage of the sulfur and nitrogen in the polymers determined by elemental analyses, and the results were summarized in Table 1. The NAC/Chitosan (mmole/g) with 10, 20, 30, 40 and 60 theoretical feedings were determined as, respectively, 0.5, 1.01, 1.45, 1.98 and 2.53; the thiol contents (mole %) of the series of Chitosan-NAC were calculated as, respectively, 8.1, 16.3, 23.4, 31.9 and 40.8%. The aqueous solubility of the Chitosan-NAC was evaluated by dissolving the test samples in deionized water until reaching their maximum concentrations. Evidently, the solubility of Chitosan-NAC was dependent on the thiol content of the polymer chain; conjugation of NAC to chitosan resulted in the introduction of highly hydrophilic $-SH$ groups onto the chitosan, thereby, disrupting its crystalline structure. The low thiol content of Chitosan-NAC-1 suggested a low ratio of $-SH$ groups and its moderate degree of disruption of the crystalline structure of chitosan, thus a low water solubility. The solubility of Chitosan-NAC increased with its thiol content, reaching at 8% maximum (Chitosan-NAC -3 and 4), then decreased. Chitosan-NAC with high thiol (i.e., 40.8%) tended to form a transparent solid gel during the dissolution process. It could thus be inferred that the introduction of a large number of $-SH$ into chitosan could enable greater structural interactions, especially the self-crosslinking of thiol groups via disulfide bond formation, thereby, influenced the solubility. Chitosan-NAC-3 and -4

appeared to have the most optimal thiol contents resulting in their relatively high solubilities.

3.2. Rheological analyses

The characteristics of *in situ* gelable hydrogel systems are epitomized by their rheological properties. Fig. 2 depicted the temporal variation of the elastic modulus (G'), the viscous modulus (G'') and the complex viscosity (η^*) of the representative Odex/Chitosan-NAC-4 (volume ratio 1:1) admixture (Fig. 2A) and the Chitosan-NAC-4 solution (3.75% w/v) which had equal concentration of Odex/Chitosan-NAC-4 admixture (Fig. 2B) at 37°C. For Odex/Chitosan-NAC-4, with G' lower than G'' , the precursor exhibited the typical behavior of viscous fluids. Both moduli elevated rapidly as gelation proceeded; the buildup rate of G' was considerably higher than that of G'' due to the formation of crosslinkings. The different elevation rates of G' and G'' led to a crossover ($t = t_{gel}$, where t_{gel} was the gel point) [33], signifying the transition of the precursor from a liquid-phase to a solid-phase. Both moduli continued to increase and eventually plateau, indicating the formation of a well-developed three-dimensional network. The η^* of the Odex/Chitosan-NAC-4 system also underwent a similar transition. At 37°C, the t_{gel} of this formulation was approximately 60 s, and its G' and η^* plateau at 2200 Pa and 300 Pa.s, respectively, at approximately 2000s.

The rheological profile of the auto-gelable thiolated chitosan hydrogels (Chitosan-NAC-4 only) was generally comparable to that of the Odex/Chitosan-NAC-4, with the exception of a considerably longer t_{gel} (1300s) and lower mechanical strength (its G' and η^* plateau at 567 Pa and 80 Pa.s, respectively, at 3600s). This gelation profile showed that, Chitosan-NAC could form hydrogel in the absence of a crosslinking reagent; however its slow reaction rate and weak mechanical strength would greatly limit its application as an *in situ* gelable hydrogel. The large disparities in the t_{gel} of the two networks (i.e., 60s and 1300s) enabled the formation of two distinct but interpenetrating networks in the same hydrogel structure, which would otherwise not be possible in a binary system. The Odex/Chitosan-NAC composition established the double network hydrogel crosslinking first via Schiff base formation, followed by disulfide bonding. This system could, therefore, solidify at body temperature rapidly, and gradually evolve into a three-dimensional interpenetrating double network over time, imparting excellent mechanical property.

The relationships between the rheological properties and the thiol content of Chitosan-NAC were investigated; the results were summarized in Table 2. The rheological properties of the hydrogels formulated with different Chitosan-NACs (the weight ratio of the two components maintained at unity) were evidently different; indicating the thiol content in Chitosan-NAC was a key contributing factor to the hydrogels' rheological properties. It could thus be deduced that both the gelation time and mechanical properties of the hydrogel could be modulated by changing the thiol content of Chitosan-NAC; either excessive or insufficient amounts of thiol groups on the Chitosan-NAC adversely affected the crosslinking reaction of the two components. When the thiol content of Chitosan-NAC was 31.9% (Chitosan-NAC-4), the mixed precursor had the shortest reaction time span ($t_{max}=2000s$) with the hydrogel formed possessing the greatest mechanical strength ($G'_{max}=2200Pa$), at a gelation time of 60s. Hypothetically, this formulation would allow sufficient amount of time for material preparation (e.g., mixing, incorporation of therapeutic agents, if relevant, etc.) and rapid gelation if an injectable formulation is to be contemplated.

3.3. Burst pressure of hydrogels

Burst strength, reflecting material cohesiveness/adhesiveness, is another important mechanical characteristic of hydrogels, especially for those that are gelable *in situ* [34–36]. The temporal burst strengths of the double network Odex/Chitosan-NAC hydrogels (Gel 3, 4

and 5) and Chitosan-NAC-4 hydrogel (a single network) were determined. All hydrogels prepared were incubated at 37 °C for 0.25, 0.5, 1, 3 and 6 hours, prior to determining their burst strengths. Incremental hydrostatic pressure was exerted on the hydrogels until failure, with the maximum pressure (burst strength) registered as the ultimate strength of the sample; the results are depicted in Fig. 3.

Compared to the auto-gelable hydrogels formulated from disulfide crosslinking (i.e., Chitosan-NAC-4), the general mechanical strength of Odex/Chitosan-NAC hydrogels was considerably higher due to Schiff base formation in concert with the interpenetrated disulfide bonding. Additionally, the rates of elevation in burst strengths were in the order of Gel 4 > Gel 3 > Gel 5 >> Chitosan-NAC-4. In the presence of Odex, all hydrogel samples (gels 3, 4 and 5) nearly reached their maximum burst strengths via developing three-dimensional interpenetrating double network in 30 minutes (0.5 hour). While after 6 hours, the burst strength of auto-gelable Chitosan-NAC-4 hydrogel was approximately 5 mmHg/mm thickness, and evidently, continued to elevate, suggesting a very slow reaction and brittleness and/or weak adhesion to substrate. Similar to the results of rheological testing, the ultimate burst strength of the Odex/Chitosan-NAC hydrogel was also in the order of Gel 4 > Gel 3 > Gel 5, which was dictated by their relevant crosslinking densities, and thus the thiol content of the Chitosan-NAC.

Collectively, the results of burst strength testing strongly corroborated with those obtained from the rheological measurement demonstrating that the mechanical and rheological properties of thiolated chitosan based hydrogels could be greatly improved by introducing the macromolecular crosslinker, Odex. The Odex/Chitosan-NAC hydrogel was mechanically strong with a short t_{gel} and reaction time span, which brought forth the possibilities of adapting it as an injection deployable *in situ* gelable material for future clinical applications.

3.4. Morphology of Odex/Chitosan-NAC hydrogels

The cross-sectional SEM images of representative lyophilized Odex/Chitosan-NAC hydrogel formulations with different thiol contents (Gels 3, 4 and 5) and the corresponding hydrogel produced from Chitosan-NAC-4 were depicted in Fig. 4. All hydrogels had porous interior structures with interconnected pores, but their pore size distributions and wall structures were obviously different, these were attributable to the crosslinking densities and material contents of the hydrogels formed. The Chitosan-NAC-4 formulation with the largest pore size (average: 300 μm) was attributable to its low crosslinking density, the loose sheet-like wall structure implicated a low mechanical strength. Conversely, the structures of all the Odex/Chitosan-NAC hydrogels possessed thick wall and were more compact. As the Odex/Chitosan-NAC hydrogels were formulated by developing double interpenetrating network structures with high material contents, they generally exhibited smaller sized pores and stronger mechanical properties. Additionally, the general pore size dimensions of the hydrogels formulated from Chitosan-NAC with different thiol contents were different; this aspect was also determined by the crosslinking densities and thus the thiol contents. Gel 4 had the smallest pore size (average: 150 μm) attributable to its high crosslinking density, which was in strong agreement with the rheological results summarized in Table 2. Since Gel 3 and 5 had lower crosslinking densities compared to Gel 4, they generally exhibited larger sized pores with weaker mechanical properties.

3.4. Swelling analysis

Fig. 5 showed the time evolution of the swelling ratio q of hydrogels. All hydrogels were submerged in PBS and their swelling ratios were determined at 0.5, 2, 6, 24 and 48 hrs. Briefly, after 2 hours of incubation, all hydrogels reached their full swollen state and they

were in the order of Gel 5 (q : 11) > Gel 3(q : 9.3) > Gel 4(q : 6.8). Gel 4 with the highest crosslinking density resulted in the minimum swelling ratio; this was in good agreement with the structural information depicted in Fig. 4.

3.5. Interaction of fibroblast and Odex/Chitosan-NAC hydrogel

Cell encapsulation was performed to explore the potential of the thiolated chitosan based hydrogels as a biomaterial; dermal fibroblast was selected as a model cell for investigation.

3.5.1. Cytotoxicity and cell viability analysis—The cytotoxicity potential, as reflected by the viability of cells encapsulated in the hydrogels (Gel 3, 4 and 5), were evaluated by MTS assays. Cells were encapsulated by hydrogels previously deposited on culture wells on day 0, and culture wells without hydrogel were used as controls. Cell viability was examined at 0, 3, 7, 14 and 28 days, and some of the results were depicted in Fig. 6. The short-term results (within 3 days, not shown) showed that there was no significant difference between the cells incubated with hydrogels and the controls, suggesting that the hydrogels did not have any adverse effect on cell growth, this could be inferred as material non-cytotoxicity ($P < 0.05$). Long-term cell culture results (up to 28 days, not shown) showed that cells in the hydrogels proliferated steadily with time and the magnitudes were comparable, this further confirmed the non-cytotoxicity of the hydrogels and it could also be inferred that the degradation byproducts of the hydrogels were non-cytotoxic. It should be noted that the controls being utilized were 2D cell culture wells and upon reaching full confluence, the cells have limited room for growth. This constraint accounted for the apparent lower cell numbers, compared to those on the 3D hydrogels, observed from day 7 and beyond. Additionally, amongst the three hydrogel formulations, Gel 4 (contained Chitosan-NAC-4) appeared to be the least amenable to cell growth; this observation was attributable to their difference in crosslinking densities. Gel 4 had the greatest crosslinking density and thus, the greatest mechanical strength, the thickest wall structure, the most compact structure and the lowest swelling ratio; these features collectively constituted a structure more resistant to cell mediated degradation, deposition of extracellular matrix (ECM) etc., thereby, impeded cell migration/infiltration into the hydrogel.

3.5.2 Cell morphology in the hydrogel—Live/Dead™ staining was performed to differentiate living cells stained with calcein-AM (green) versus the dead cells stained with ethidium homodimer (red) by fluorescence microscopy. Fig. 7 depicted the cells residing in the 5% Odex/2.5% Chitosan-NAC-4 (Volume ratio 1:1) hydrogel formulation after Live/Dead™ staining. Cells residing inside the hydrogel assumed a round conformation during the first 7 days (Fig. 7A), and approximately 70% of the cells were alive. After 14 days, cells started to assume their typical conformation (Fig. 7B) with the overwhelming majority (>70%) of them alive. This suggested that the cells were adapting to the new hydrogel "environment"; it is known that fibroblasts deposit extracellular matrix on polymer matrices [39, 40]. The extracellular matrix deposited on the hydrogels modulated its properties rendered it more favorable for cells to regulate their behavior including morphology, functionality and cell-cell interactions [41].

3.5.3. Degradation of the hydrogels in a cell culture model—Cell mediated degradation studies for hydrogel formulations, Gels 3, 4 and 5, were conducted by monitoring their weight losses in the presence of cells, the results were depicted in Fig. 8. Apparently, all hydrogels underwent relatively fast initial degradation during the first 2 weeks; it was followed by a more moderate phase. The pace of degradation was in the order of Gel 5 > Gel 3 > Gel 4; this pattern of degradation kinetics reflected the stabilities of the hydrogels and they were in the order of Gel 4 > Gel 3 > Gel 5. In general, the degradation behavior of hydrogels is dependent on the crosslinking density [38]. The extent of

crosslinking implicates the stability of the hydrogel; greater degrees of crosslinking produce hydrogels that are more stable. As shown above, Gel 4 had the highest crosslinking density and it was the most resistant to degradation.

3.5.3. Subdermal implantation of hydrogels—The implant sites of the mice were examined immediately after euthanasia (7 and 28 days, respectively). The needle puncture injuries of the animals of both groups were completely healed by day 7, as indicated by wound closure, and they could not be easily identified; this suggested normal healing; moreover, there was neither any observable abnormality nor hair loss on the skin surface, implicating the non-cytotoxicity of the injected hydrogels (not shown). The gross appearance of the tissues surrounding the implanted hydrogels did not show any signs of edema, redness or tissue necrosis (not shown); this suggested that the hydrogels residing inside the subdermal pouches did not induce extensive inflammatory response. The histopathology depicted in Figure 9A showed that the fibrous capsules, typically surrounding implants, were thin suggesting the presence of the hydrogels produced only very mild tissue responses; there was no evidence of extensive presence of inflammatory cells, further corroborating the initial gross examination. In contrast, the tissues adjoining the implanted synthetic poly-lactide-co-glycolide (i.e., Vicryl™, as benchmarks, not shown) were surrounded by considerably thicker fibrous capsules. Moreover, the surface/boundary of the hydrogel in direct contact with the tissue was intact and distinctive, with no evidence of cell infiltration; these observations collectively indicated the resistance of the hydrogel to biodegradation. This feature is a distinct contrast to most hydrogels formulated from minimally modified natural materials which tend to degrade relatively rapidly upon *in vivo* implantation. The histopathology of the implant sites after 28 days (Figure 9B) highly resembled those of the day 7, the fibrous tissue surrounding the implanted hydrogel was noticeably thicker and denser; however, there was no evidence of extensive presence of inflammatory cells or foreign body giant cells. Likewise, cells did not infiltrate into the hydrogel and it clearly maintained a fully intact boundary interfacing the surrounding tissue further indicating non-cytotoxicity and lack of biodegradation.

We had previously demonstrated cell/tissue mediated degradation/erosion of a similar *in situ* gelable but single network hydrogel composed of Odex and carboxyethyl chitosan (CEC), they were fully degraded in animal models within 4 weeks after implantation [42,43]; apparently, substituting Chitosan-NAC for CEC greatly increased the stability and durability of the hydrogel formed both *in vitro* and *in vivo*. These results suggested the disulfide bond inter-crosslinkings formed as the second network is the major factor contributing to the resistance to degradation. Disulfide bonds are known to be reversible under weak acidic condition; the neutral physiological pH further contributes to the stability of the disulfide bonds formed [29]. It has also been shown that disulfide bonds are very stable and the hydrogels formed via this mode of crosslinking are resistant to hydrolysis [30]. In fact, the *in vivo* stability observed in this investigation is consistent with a previously reported pre-formed film prepared by the crosslinking of sulfhydryl modified hyaluronan and stabilized by hydrogen peroxide treatment [30]. It should be noted that that the *in vitro* results (Fig. 8) showed that up to 25% of the hydrogel (Gel 4) was degraded by week 4, which did not fully reflect the same hydrogel's lack of degradation *in vivo* after implantation. We postulate that this disparity was due to the availability of excess water in the *in vitro* cell culture, which permitted the hydrogel to swell to multiple times of its original volume, this in turn, facilitated cell penetration and diffusion of the degradative enzymes they secreted, thereby, hastening the break down. In contrast, only very limited free water was available to the hydrogel upon implantation, which greatly limited its swelling *in vivo*. The hydrogel's denser structure in concert with the double network crosslinking molecular organization rendered it highly resistant to degradation upon implanted *in vivo*.

All the *in vivo* and *in vitro* results demonstrated that Odex/Chitosan-NAC with interpenetrating double networks is an effective hydrogel system to enhance the mechanical strengths, and thus, increase their resistance to degradation, which indicated that thiolated chitosan hydrogels have great potential as an *in situ* formable biomaterial for clinically related applications where mechanical strength, durability and fast gelation are the essential requirements.

Conclusion

A class of binary *in situ* gelable double-interpenetrating network hydrogels, composed of minimally modified natural GRAS materials, oxidized dextran (Odex) and thiolated chitosan (Chitosan-NAC), has been formulated without the need of any small molecule crosslinker. The interpenetrating network structure is created by disulfide bonds and Schiff base formations, respectively. The results of burst strength testing strongly corroborate with the rheological measurements; it demonstrates that the Odex/Chitosan-NAC hydrogel is mechanically strong with a short t_{gel} and reaction time span, which brings forth the possibilities of adapting it as an injection deployable *in situ* gelable material for future clinical applications. Short and long-term viability tests of the Odex/Chitosan-NAC hydrogel using fibroblast-mediated *in vitro* models show that both the hydrogel and its degradation byproducts are non-cytotoxic. *In vivo* results from subdermal implantation demonstrate the low inflammatory potential of the hydrogel and its resistance to degradation. Collectively, the results suggest that the double interpenetrating network Odex/Chitosan-NAC hydrogel system has great potential as an *in situ* formable biomaterial for clinically related applications where mechanical strength, durability and fast gelation are the essential requirements.

Acknowledgments

This study was supported by the National Institutes of Health (NS070331); partial support was also provided DK068401 and an ECAT (Enhanced Center for Advanced Technology) grant from NYSTAR (New York Foundation for Science, Technology and Innovation) administered by the Center for Biotechnology of SUNY-Stony Brook.

References

1. Shu XZ, Liu YC, Palumbol FS, Luo Y, Prestwich GD. In situ crosslinkable hyaluronan hydrogels for tissue engineering. *Biomaterials*. 2004; 25:1339–1348. [PubMed: 14643608]
2. Taleb MFA, Abdel-Aal SE, El-Kelesh NA, Hegazy EA. Adsorption and controlled release of Chlorotetracycline HCl by using multifunctional polymeric hydrogels. *Eur. Poly. J.* 2007; 43(2):468–477.
3. Fournier E, Passirani C, Montero-Menei CN, Benoit JP. Biocompatibility of implantable synthetic polymeric drug carriers: focus on brain biocompatibility. *Biomaterials*. 2003; 24(19):3311–3331. [PubMed: 12763459]
4. Lee KY, Mooney DJ. Hydrogels for tissue engineering. *Chem. Rev.* 2001; 101:1869–1879. [PubMed: 11710233]
5. Tan H, Chu CR, Payne KA, Marra KG. Injectable in situ forming biodegradable chitosan-hyaluronic acid based hydrogels for cartilage tissue engineering. *Biomaterials*. 2009; 30(13):2499–2506. [PubMed: 19167750]
6. Weng L, Chen X, Chen W. Rheological properties of in situ crosslinkable hydrogels from dextran and chitosan derivatives. *Biomacromolecules*. 2007; 8:1109–1115. [PubMed: 17358076]
7. Mandal BB, Kapoor S, Kundu SC. Silk fibroin/polyacrylamide semi-interpenetrating network hydrogels for controlled drug release. *Biomaterials*. 2009; 30(14):2826–2836. [PubMed: 19203791]

8. Wang X, Zheng C, Wu Z, Teng D, Zhang X, Wang Z, Li C. Chitosan-NAC nanoparticles as a vehicle for nasal absorption enhancement of insulin. *J. Biomed. Mater. Res. B Appl. Biomater.* 2009; 88(1):150–161. [PubMed: 18618466]
9. Dos Santos JF, Alvarez-Lorenzo C, Silva M, Balsa L, Couceiro J, Torres-Labandeira JJ, Concheiro A. Soft contact lenses functionalized with pendant cyclodextrins for controlled drug delivery. *Biomaterials.* 2009; 30(7):1348–1355. [PubMed: 19064285]
10. Rafat M, Li F, Fagerholm P, Lagali NS, Watsky MA, Munger R, Matsuura T, Griffith M. PEG-stabilized carbodiimide crosslinked collagen-chitosan hydrogels for corneal tissue engineering. *Biomaterials.* 2008; 29(29):3960–3972. [PubMed: 18639928]
11. Weng L, Gouldstone A, Wu Y, Chen W. Mechanically strong double network photocrosslinked hydrogels from N, N-dimethylacrylamide and glycidyl methacrylated hyaluronan. *Biomaterials.* 2008; 29(14):2153–2163. [PubMed: 18272215]
12. Boucard N, Viton C, Agay D, Mari E, Roger T, Chancerelle Y, Domard A. The use of physical hydrogels of chitosan for skin regeneration following third-degree burns. *Biomaterials.* 2007; 28:3478–3488. [PubMed: 17482258]
13. Song F, Zhang LM, Shi JF, Li NN. Novel casein hydrogels: formation, structure and controlled drug release. *Colloids. Surf. B Biointerfaces.* 2010; 79(1):142–148. [PubMed: 20434318]
14. Chau Y, Luo Y, Cheung AC, Nagai Y, Zhang S, Kobler JB, Zeitels SM, Langer R. Incorporation of a matrix metalloproteinase-sensitive substrate into self-assembling peptides—a model for biofunctional scaffolds. *Biomaterials.* 2008; 29(11):1713–1719. [PubMed: 18192002]
15. Ramseyer P, Micol LA, Engelhardt EM, Osterheld MC, Hubbell JA, Frey P. In vivo study of an injectable poly (acrylonitrile)-based hydrogel paste as a bulking agent for the treatment of urinary incontinence. *Biomaterials.* 2010; 31(17):4613–4619. [PubMed: 20303170]
16. Liao H, Zhang H, Chen W. Differential physical, rheological, and biological properties of rapid *in situ* gelable hydrogels composed of oxidized alginate and gelatin derived from marine or porcine sources. *J. Mater. Sci. Mater. Med.* 2009; 20(6):1263–1271. [PubMed: 19184370]
17. Gutowska A, Jeong B, Jasionowski M. Injectable gels for tissue engineering. *Anat. Rec.* 2001; 263:342–349. [PubMed: 11500810]
18. Jeong B, Bae YH, Lee DS, Kim SW. Biodegradable block copolymers as injectable drug-delivery systems. *Nature.* 1997; 388:860–862. [PubMed: 9278046]
19. Bryant SJ, Anseth KS. The effects of scaffold thickness on tissue engineered cartilage in photocrosslinked poly (ethylene oxide) hydrogels. *Biomaterials.* 2001; 22:619–626. [PubMed: 11219727]
20. Ta HT, Dass CR, Dunstan DE. Injectable chitosan hydrogels for localised cancer therapy. *J. Control. Release.* 2008; 126(3):205–216. [PubMed: 18258328]
21. Yasuda K, Ping GJ, Katsuyama Y, Nakayama A, Tanabe Y, Kondo E, Ueno M, Osada Y. Biomechanical properties of high-toughness double network hydrogels. *Biomaterials.* 2005; 26(21):4468–4475. [PubMed: 15701376]
22. Tirumala VR, Tominaga T, Lee S, Butler PD, Lin EK, Gong JP, Wu WL. Molecular model for toughening in double-network hydrogels. *J. Phys. Chem. B.* 2008; 112(27):8024–8031. [PubMed: 18558754]
23. Tanabe Y, Yasuda K, Azuma C, Taniguro H, Onodera S, Suzuki A, Chen YM, Gong JP, Osada Y. Biological responses of novel high-toughness double network hydrogels in muscle and the subcutaneous tissues. *J. Mater. Sci. Mater. Med.* 2008; 19(3):1379–1387. [PubMed: 17914620]
24. Myung D, Waters D, Wiseman M, Duhamel PE, Noolandi J, Ta CN, Frank CW. Progress in the development of interpenetrating polymer network hydrogels. *Polym. Adv. Technol.* 2008; 19(6): 647–657. [PubMed: 19763189]
25. Topuz F, Okay O. Formation of hydrogels by simultaneous denaturation and cross-linking of DNA. *Biomacromolecules.* 2009; 10(9):2652–2661. [PubMed: 19658412]
26. Werle M, Bernkop-Schnürch A. Thiolated chitosans: useful excipients for oral drug delivery. *J. Pharm. Pharmacol.* 2008; 60(3):273–281. [PubMed: 18284806]
27. Hombach J, Hoyer H, Bernkop-Schnürch A. Thiolated chitosans: development and in vitro evaluation of an oral tobramycin sulphate delivery system. *Eur. J. Pharm. Sci.* 2008; 33(1):1–8. [PubMed: 17980561]

28. Schmitz T, Grabovac V, Palmberger TF, Hoffer MH, Bernkop-Schnürch A. Synthesis and characterization of a chitosan-N-acetyl cysteine conjugate. *Int. J. Pharm.* 2008; 347(1–2):79–85. [PubMed: 17681439]
29. Shu XZ, Liu YC, Luo Y, Roberts MC, Prestwich GD. Disulfide Cross-Linked Hyaluronan Hydrogels. *Biomacromolecules.* 2002; 3:1304–1311. [PubMed: 12425669]
30. Liu Y, Shu XZ, Prestwich G. Biocompatibility and stability of disulfide crosslinked hyaluronan films. *Biomaterials.* 2005; 26:4737–4746. [PubMed: 15763253]
31. Krauland AH, Hoffer MH, Bernkop-Schnürch A. Viscoelastic preoerties of a new in situ gelling thiolated chitosan conjugate. *Drug. Dev. Ind. Pharm.* 2005; 31:885–893. [PubMed: 16306000]
32. Weng L, Romanov A, Rooney J, Chen W. Non-cytotoxic, in situ gelable hydrogels composed of N-carboxyethyl chitosan and oxidized dextran. *Biomaterials.* 2008; (29):3905–3913. [PubMed: 18639926]
33. Zhang HW, Qadeer A, Mynarcik D, Chen W. Delivery of rosiglitazone from an injectable triple interpenetrating network hydrogel composed of naturally derived materials. *Biomaterials.* 2011; 32(3):890–898. [PubMed: 20947157]
34. Winter HH, Chambon F. Analysis of linear viscoelasticity of a crosslinking polymer at the gel point. *J. Rheol.* 1986; 30:367–382.
35. Kobayashi H, Sekine T, Nakamura T, Shimizu Y. In vivo evaluation of a new sealant material on a rat lung air leak model. *J. Biomed. Mater. Res.* 2001; 58(6):658–665. [PubMed: 11745518]
36. Shazly TM, Artzi N, Boehning F, Edelman ER. Viscoelastic adhesive mechanics of aldehyde-mediated soft tissue sealants. *Biomaterials.* 2008; 29(35):4584–4591. [PubMed: 18804861]
37. Wallace DG, Cruise GM, Rhee WM, Schroeder JA, Prior JJ, Ju J, Maroney M, Duronio J, Ngo MH, Estridge T, Coker GC. A tissue sealant based on reactive multifunctional polyethylene glycol. *J. Biomed. Mater. Res.* 2001; 58(5):545–555. [PubMed: 11505430]
38. Lee KY, Bouhadir KH, Mooney DJ. Degradation behavior of covalent crosslinked poly(aldehyde guluronate) hydrogels. *Macromolecules.* 2000; 33:97–101.
39. Tamada Y, Ikada Y. Fibroblast growth on polymer surface and biosynthesis of collagen. *J. Biomed. Mater. Res.* 2004; 28:783–789. [PubMed: 8083246]
40. Halfter W, Liverani D, Vigny M, Monard D. Deposition of extracellular matrix along the pathways of migrating fibroblasts. *Cell Tissue Res.* 1990; 262:467–481. [PubMed: 1706644]
41. Mo XM, Xu CY, Kotaki M, Ramakrishna S. Electrospun P(LLA-CL) nanofiber: a biomimetic extracellular matrix for smooth muscle cell and endothelial cell proliferation. *Biomaterials.* 2004; 25:1883–1890. [PubMed: 14738852]
42. Yuan Z, Zakhaleva J, Ren H, Liu J, Chen W, Pan Y. Noninvasive and High-resolution Optical Monitoring of Healing of Diabetic Dermal Excisional Wounds Implanted with Biodegradable in situ Gelable Hydrogels. *Tissue Eng. Part C Methods.* 2010; 16(2):237–247. [PubMed: 19496703]
43. Falabella CA, Melendez M, Weng LH, Chen W. Novel macromolecular crosslinking hydrogel to reduce intra-abdominal adhesions. *J. Surg. Res.* 2010; 159(2):772–778. [PubMed: 19481223]

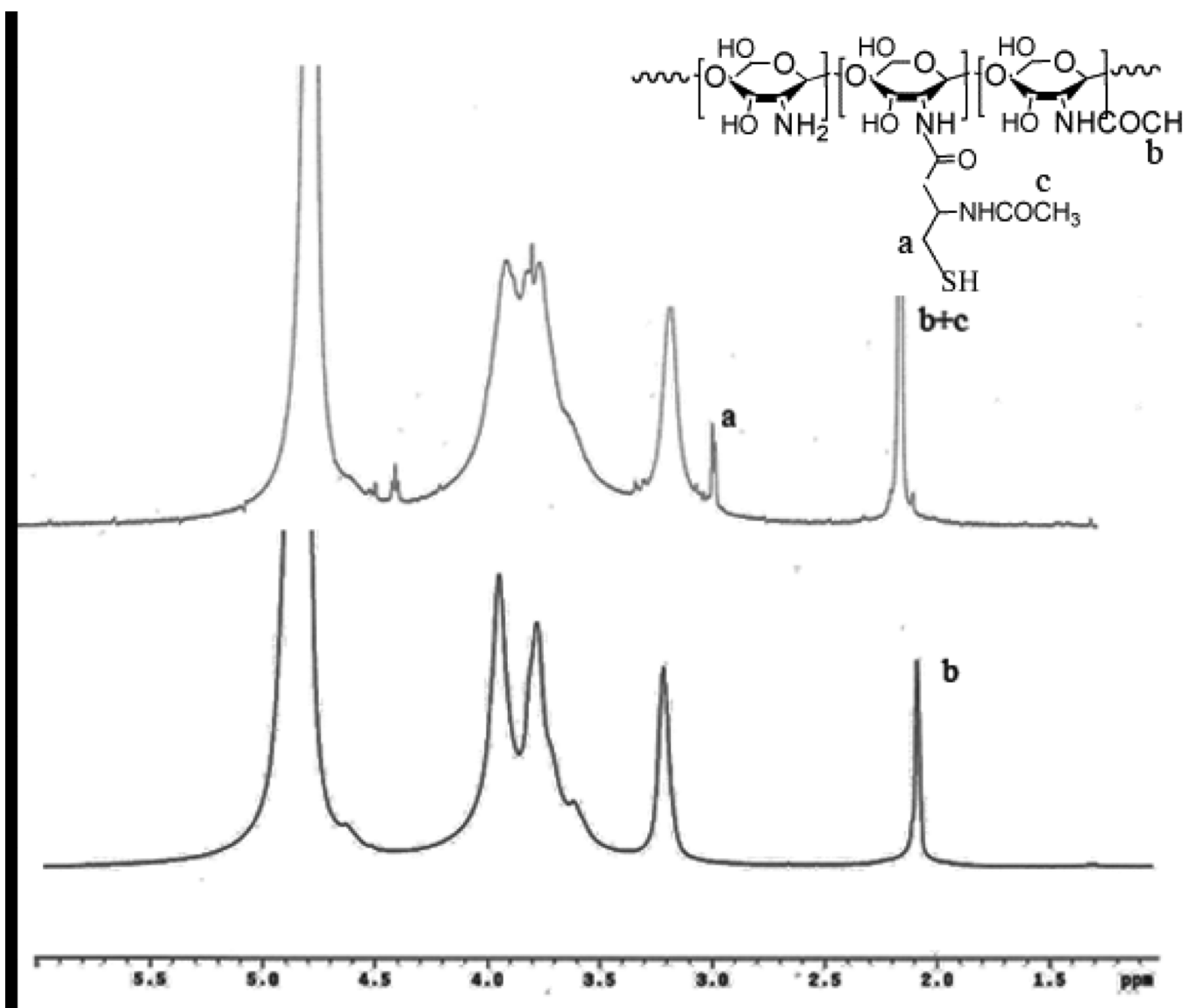


Fig. 1.
The ^1H NMR spectrum of Chitosan-NAC

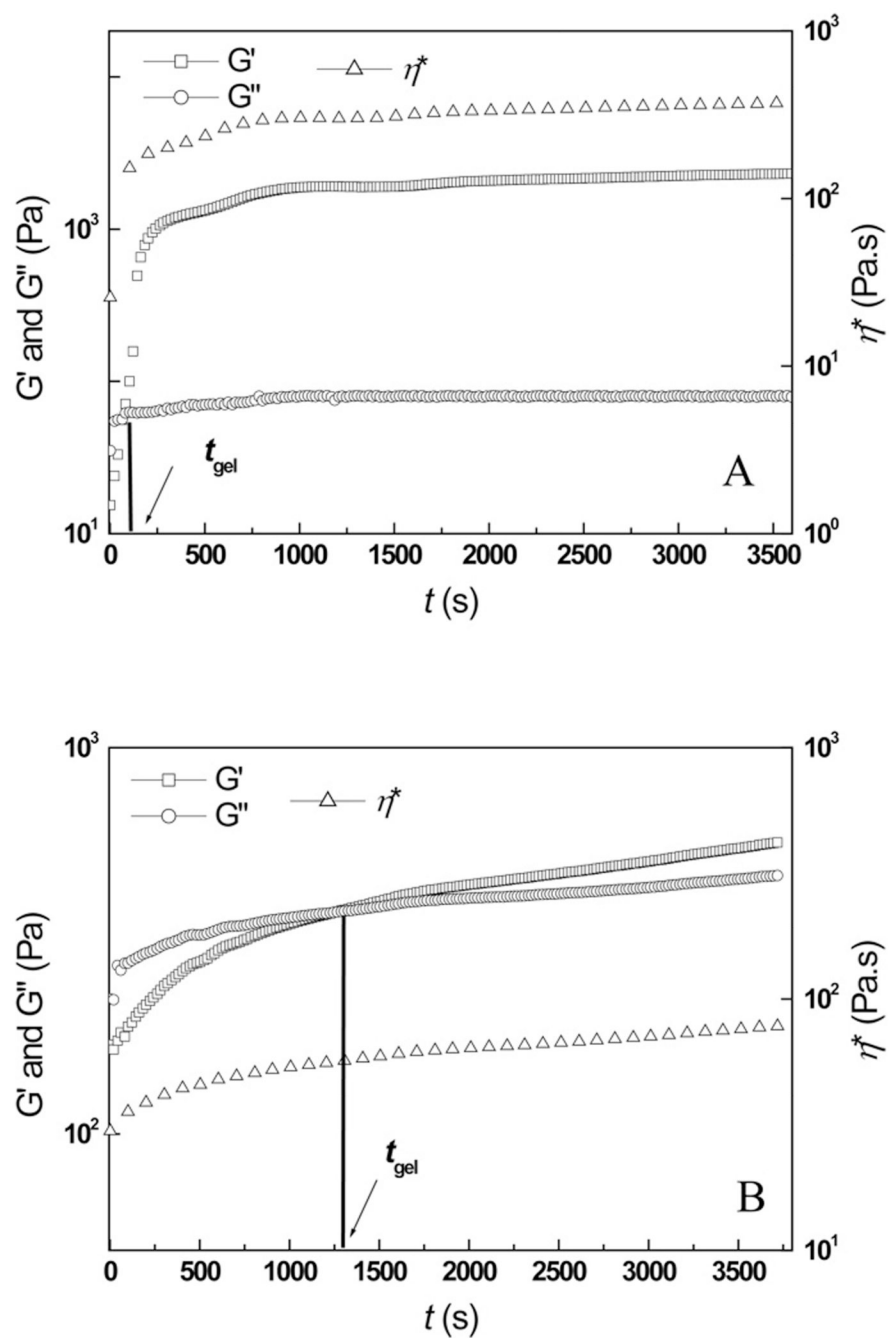


Fig. 2. The time evolution of the storage modulus (G'), the loss modulus (G'') and the complex viscosity (η^*) of: (A) Odex/Chitosan-NAC-4 (weight ratio 1:1) hydrogel, and (B) the corresponding Chitosan-NAC-4 hydrogel formed by self-crosslinking. G' and G'' crossover is denoted as t_{gel} (gelation point)

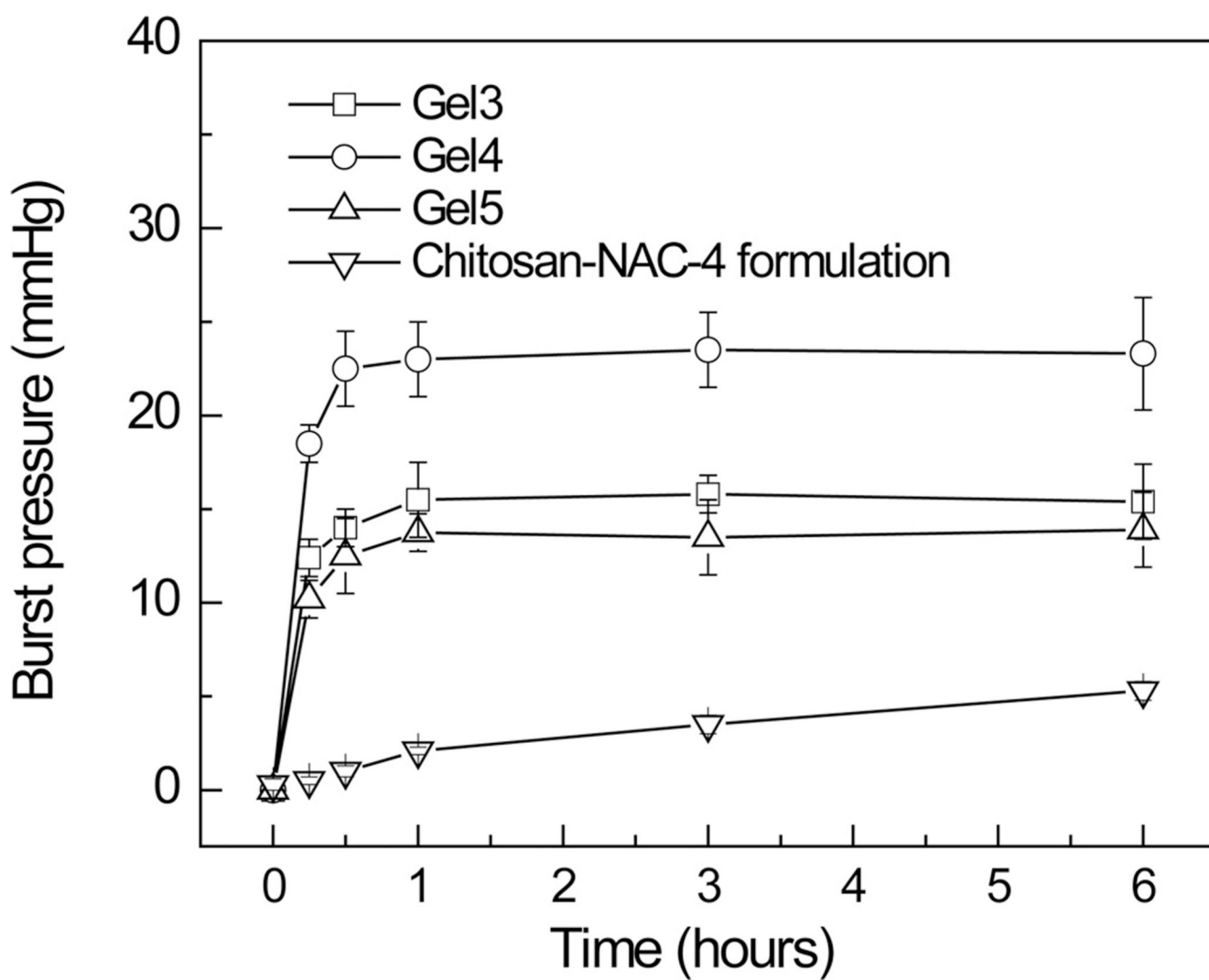
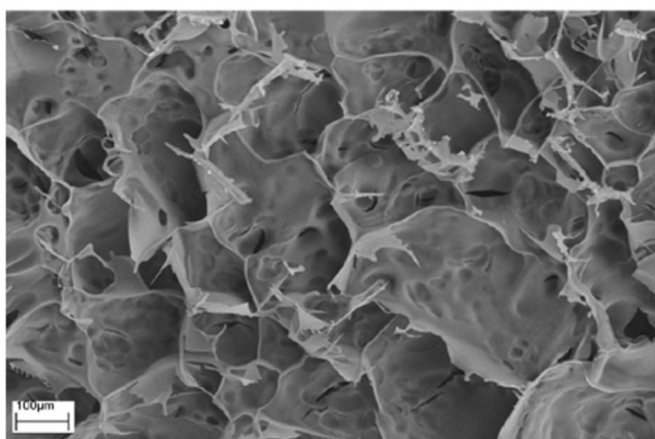
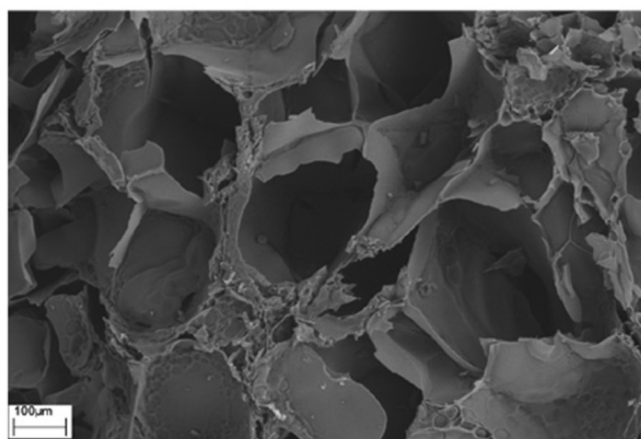


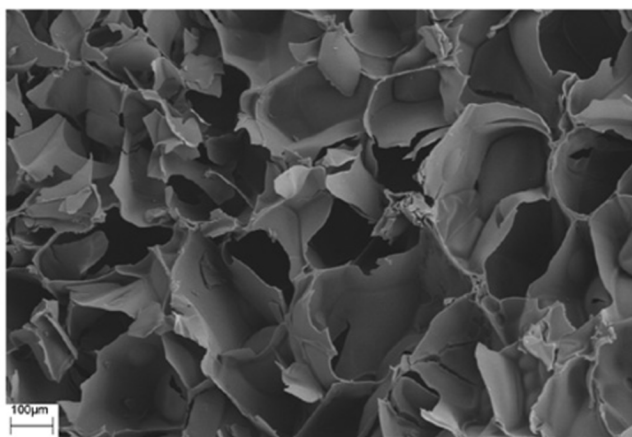
Fig. 3. The time evolution of burst pressure of the double network Odex/Chitosan-NAC hydrogels and the single network Chitosan-NAC-4 hydrogel.



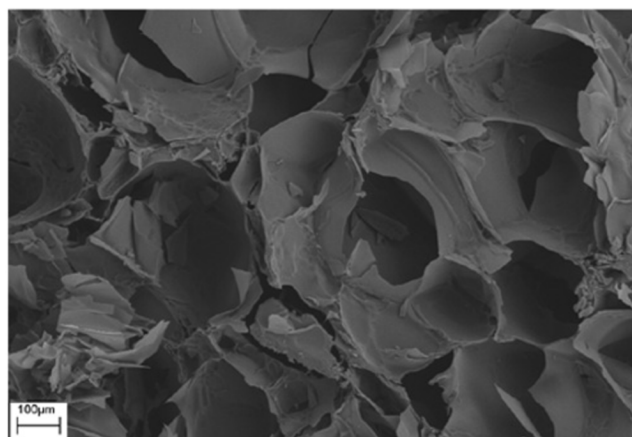
Chitosan-NAC-4 formation



Gel 3



Gel 4



Gel 5

Fig. 4. The cross-sectional SEM images of Odex/Chitosan-NAC hydrogel formulations (Gel 3, Gel 4 and Gel 5) composed of Chitosan-NAC with different thiol contents, and the hydrogel formed by self-crosslinking of Chitosan-NAC-4.

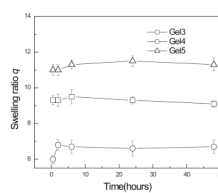


Fig. 5. The time evolution of swelling ratio q of hydrogels formulated from Chitosan-NAC with different thiol contents

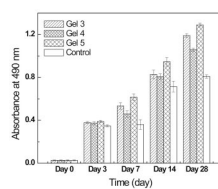


Fig. 6.
The viabilities of cells encapsulated by various hydrogel formulations.

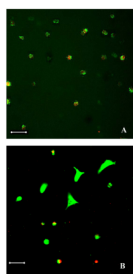


Fig. 7. Live/dead™ staining of cells entrapped in Odex/Chitosan-NAC hydrogel (Gel 4): (A) day 7, and (B) day 14. Green: live cells, and red: dead cells
Scale bar: 50 μ m

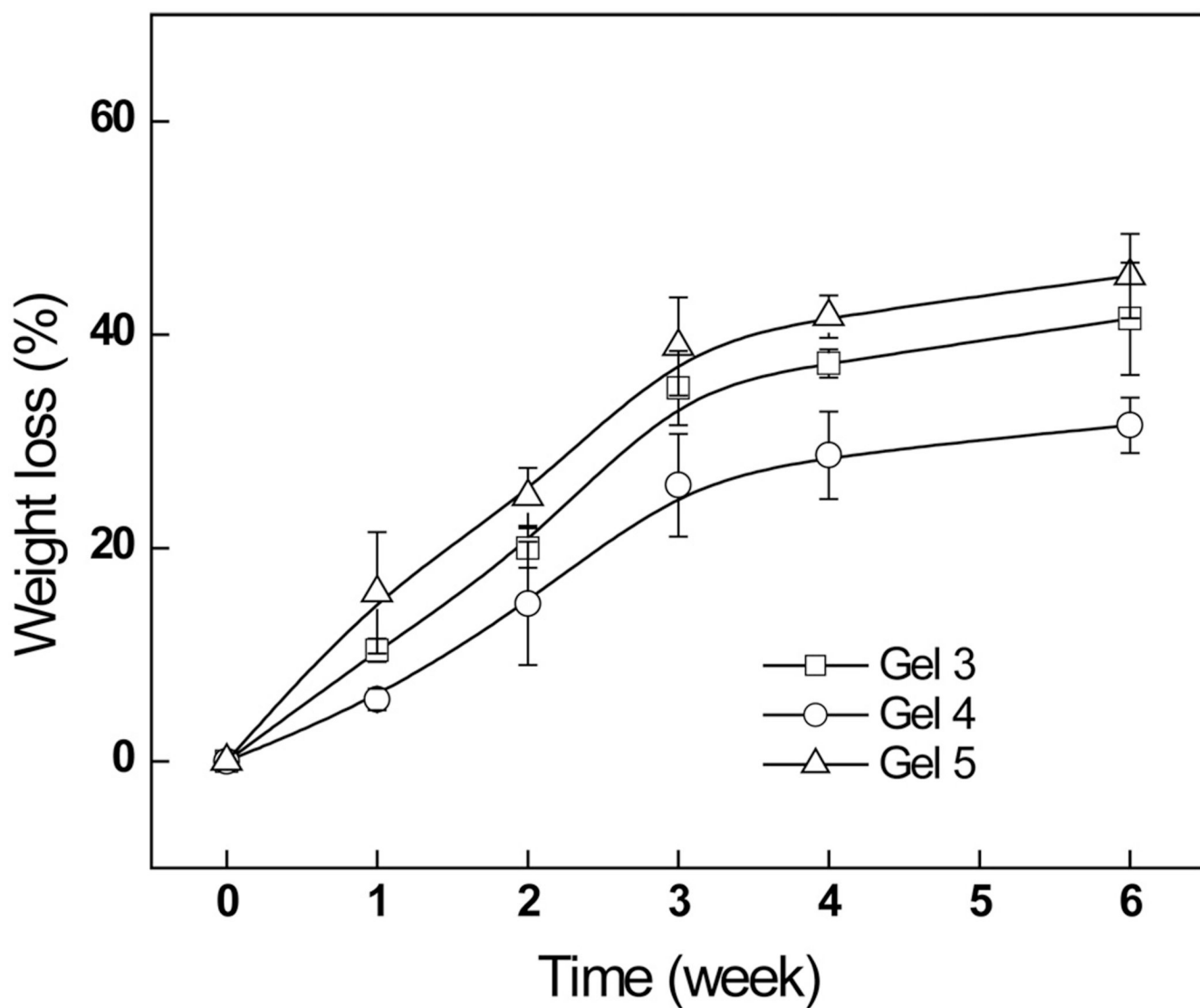


Fig. 8.
The weight loss of Odex/Chitosan-NAC hydrogels formulated from Chitosan-NACs, with different thiol contents, in PBS.

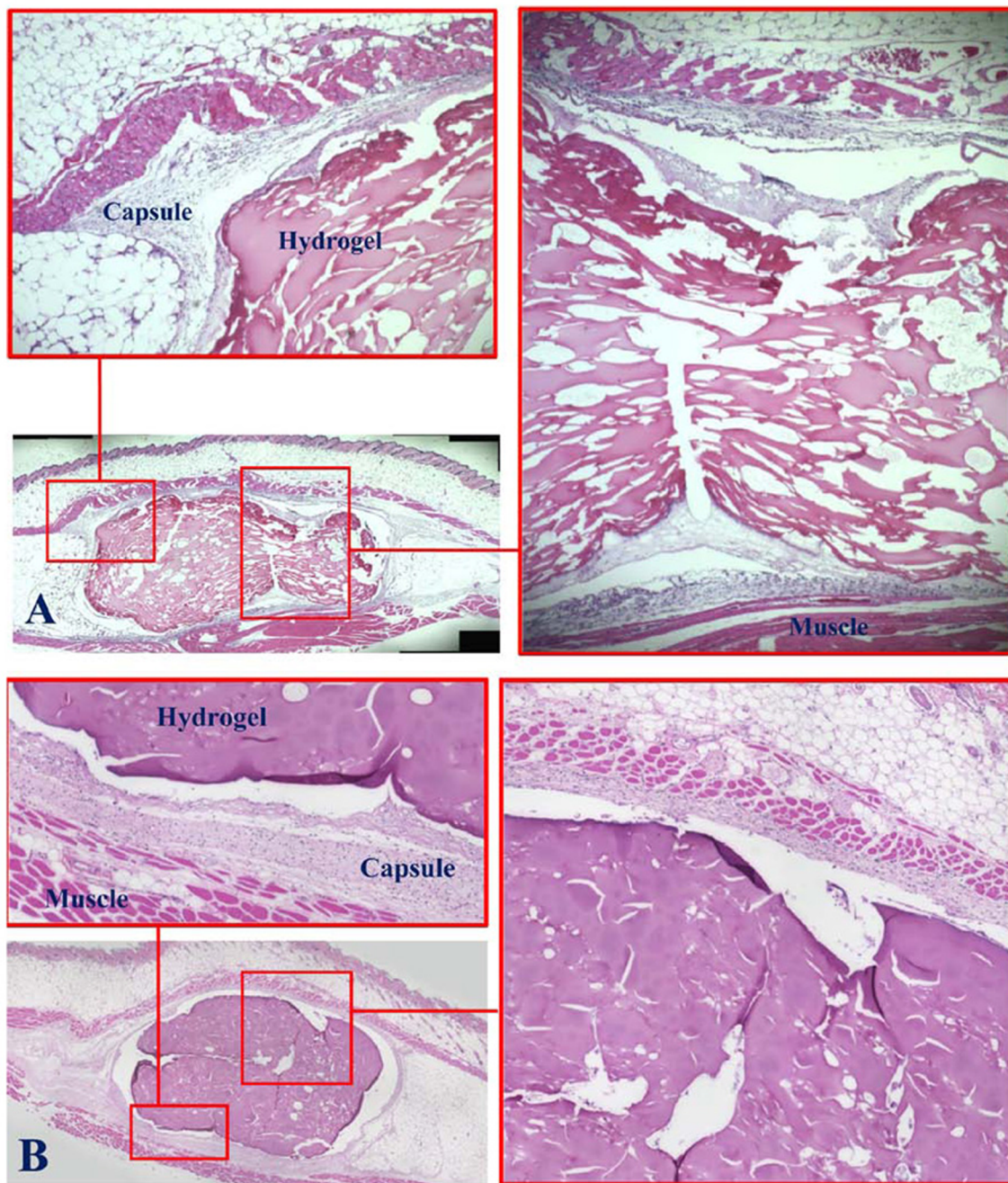
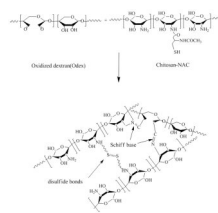


Fig. 9. Subdermal injection of Odex/Chitosan-NAC into mice. Duration: (A) 7 days, and (B) 28 days. The presence of hydrogels appear to have induced only very mild tissue response and it was reflected by the thin fibrous capsules surrounding the implants and the lack of extensive presence of inflammatory cells and foreign body giant cells.



Scheme 1.
Schematic representation of the formation of the Odex/Chitosan-NAC hydrogel

Table 1

The characteristics of Chitosan-NAC produced from different feed ratios of NAC/Chitosan

| Samples | Feeding NAC/Chitosan (mmole/g) | Obtained NAC/Chitosan* (mmole/g) | % mole of Thiol groups | Maximum aqueous solubility (%) |
|-----------------|--------------------------------|----------------------------------|------------------------|--------------------------------|
| Chitosan-NAC -1 | 10.0 | 0.50 | 8.1 | 2.5 |
| Chitosan-NAC -2 | 20.0 | 1.01 | 16.3 | 5.0 |
| Chitosan-NAC -3 | 30.0 | 1.45 | 23.4 | 8.0 |
| Chitosan-NAC -4 | 40.0 | 1.98 | 31.9 | 8.0 |
| Chitosan-NAC-5 | 60.0 | 2.53 | 40.8 | 5.0 |

* determined by elemental analysis

Table 2

The physicochemical properties of Odex/Chitoan-NAC hydrogels

| Sample | Thiol content (mol %) | t_{gel} (s) | t_{max} (s) | G'_{max} (Pa) |
|--------|-----------------------|----------------------|----------------------|------------------------|
| Gel 1 | 8.1 | <30 | 4600 | 600 |
| Gel 2 | 16.3 | 45 | 3000 | 1500 |
| Gel 3 | 23.4 | 60 | 2600 | 1800 |
| Gel 4 | 31.9 | 60 | 2000 | 2200 |
| Gel 5 | 40.8 | <30 | 4000 | 1350 |

The concentrations of Odex and Chitosan-NAC were 5 and 2.5 %, respectively